IJBBE International Journal of Biophotonics & Biomedical Engineering Vol. 3, No. 2, Summer-Fall, 2023

Research Article

Automatic design and 3D segmentation of mandible bone using CNN algorithm via exclusive GUI

Sh. Mohammadi [a], N. Mehradkia [a*], and S.A. Mousavi [a]

a Department of Mechanical Engineering, Najafabad Branch, Islamic Azad University, Isfahan, Iran.

***Corresponding author: nadia.mdkia@gmail.com**

DOI: 10.30495/ijbbe.2024.1997685.1037

ABSTRACT

Received: Nov. 15, 2023, Revised: Jan. 10, 2024, Accepted: Jan. 16, 2024, Available Online: Feb. 5, 2024

Nowadays, scientists are looking to decrease dental faults by presenting new approaches. It is obvious that comprehensive information about the anatomic position of the inferior alveolar neural canal is essential to have the most ideal mandible surgery or systemic tooth implant. Accordingly, we present a new approach in this article that can be used to have 3D segmentation and recognition of the mentioned canal in mandible by CBCT image. This approach includes two main steps. In the first step, we train a full convolutional 3D net (FCN) to reach the ability of section recognition, which can recognize the relevant area of the mandible bone. In the next step, we define a 3D U-net, which is similar to FCN, to segment the inferior Alveolar neural (IAN) canal from the lower jaw. Evaluated on publicly available datasets, our method achieved an average Dice coefficient of 86.61%.

KEYWORDS

Alveolar neural canal, CBCT, FCN, Mandible, Segmentation, U-net.

I. INTRODUCTION

In dental fields, accurate information about mandible bone can be effective in having error-free surgery and preventing tissue harm. Since advanced medical imaging including CT and CBCT, is considered one of the best information references in medical fields, it can be discovered by a technical comparison between them, that CBCT images can present high-quality outcomes for precise mandible segmentation because it is exclusively for mouth and teeth in high accuracy [1]. On the other hand, after this segmentation, the size and dimension of the mandible bone and also the exact location of the IAN canal can be recognized. Therefore, the orthognathic surgeon can be able to plan for having surgeries in a more accurate and low-risk status.

Most segmentations in recognition systems are performed in manual mode by dentists which not only is time-consuming but also has outcomes with a high range of errors. In this article, we present an automatic segmentation of the IAN canal in mandible bone which includes two steps; In the first one, the

localization process, and in the second one segmentation process is performed. The localization process will be done for recognition of the region of the mandible and the second process will be done for 3D segmentation of the IAN canal.

A lot of different techniques for tissue segmentation via medical images have been discovered up to now. For example, Lloréns and his colleagues segmented the Alveolar canal from mandible bone by using a phase connection method via CT images in two dimensions [2].

Also, Kroon could do segmentation of the Alveolar canal by using CT images, the AAM algorithm, and the ASM algorithm. This process was done through a statistic model in manual mode. The mentioned segmentation was performed in two dimensions and was able to recognize any disorder in the IAN canal of the mandible [3].

Machine learning-based methods have been used a lot in variable fields including analysis and segmentation of images. For example, Keatmanee and his colleagues segmented the Alveolar canal of the mandible by using an active contour algorithm which is one of the machine learning algorithms. This segmentation was performed by CT images in two dimensions [4]. It is worth mentioning that among different techniques of machine learning, the Deep learning method has attracted a lot of attention in the analysis and segmentation of medical images in recent years because it has a high degree of accuracy in this context. In comparison with other methods, one of the newest structures of this technique is U-net, which Olaf Ronneberger and his friends used to do 2D segmentation of medical images in a fast and practical mode [5]. The U-net structure has been used more than others in medical research. For instance, Wang and his colleagues could segment the jaw bone from the head and neck by CT image and this structure. They could define the precise location of the mandible bone [6].

In this article, we introduce a method for 3D segmentation of the IAN canal from mandible bone via CBCT images. As the first step, we train a 3D regression (FCN) to localize and define the ideal area in the jaw region. Subsequently, we do segmentation of the canal by 3D U-net, and also as the last step, we define a specific GUI to increase the efficiency of research in a way that will present the mentioned process in a format of exclusive and unique program. At the end, we will present experimental results to have a better evaluation.

II. MATERIAL AND METHODS

Since CBCT data are not the same in terms of quality, resolution, and other details, we used some techniques to minimize their differences especially for increasing their quality and decreasing their gray level discrepancies [7]. This process is called preprocessing which will be explained in detail in the following. Also, all the steps of our method are shown in the flowchart below briefly.

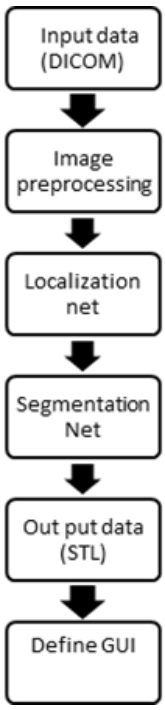

Fig. **1** Flowchart of method steps

A. *Preprocessing*

In addition to different quality levels, all CBCT images include different frequency interferences which should be minimized as much as possible to be practical for segmentation. Thus, we use two algorithms to improve data. Histogram and low-pass filtering are these algorithms. Low-pass filtering can cause diminishing interferences by passing through the low-frequency pixels and changing high-frequency pixels to have more uniform data [9].

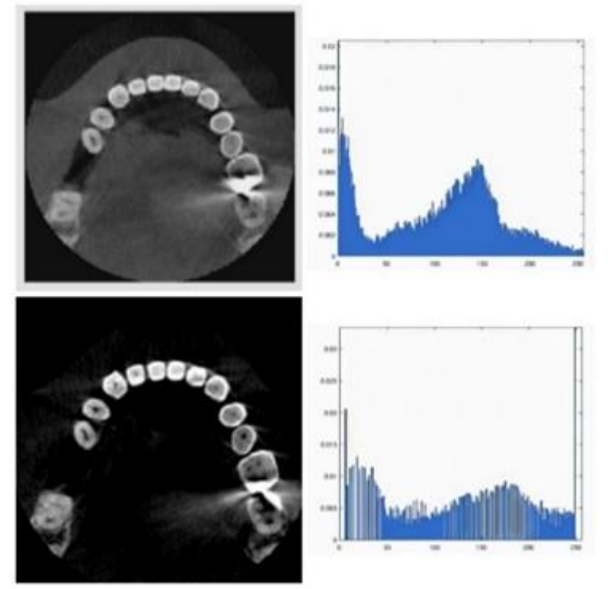

Fig. **2** View of histogram function for CBCT image, (upper image is the original histogram before equalization and the other one is the equalized one.)

We use Gaussian smoothing to remove noisy pixels and smoothing images. Gaussian smoothing is a type of low-pass filter. Low-pass filters allow low-frequency components (such as smooth variations) to pass through while attenuating or reducing the high-frequency components (such as noise or rapid changes). Gaussian smoothing achieves this by convolving the image with a Gaussian kernel, where the shape of the kernel is determined by a Gaussian function. The Gaussian function emphasizes the central pixels more and gradually reduces the emphasis on the outer pixels, resulting in a blurring or smoothing effect. Therefore, Gaussian smoothing acts as a low-pass filter by reducing noise and high-frequency details while preserving the overall structure and lower-frequency components of the image [9]. Also, histogram equalization is a technique used to improve the contrast of images by redistributing the pixel intensity values. In CBCT images, histogram equalization can be used to improve the contrast between different structures and tissues in the image.

CBCT images are often affected by noise and artifacts that can reduce the contrast between different structures in the image. Histogram equalization can help to enhance the contrast by stretching the intensity values across the entire range of the image. This results in a more even distribution of pixel intensities, which can improve the visibility of structures that were previously difficult to see. Furthermore, histogram equalization can also help to reduce the effect of scatter radiation in CBCT images. Scatter radiation can cause artifacts and reduce the contrast in the image, but histogram equalization can help to compensate for this effect by redistributing the pixel intensities.

Overall, histogram equalization is a useful technique for improving the contrast of CBCT images, making it easier to visualize and diagnose different structures and tissues in the image [8].

B. *Localization Net*

According to previous work [10], we also consider the mandible region localization as a regression problem. In a way, we determine a cube to show the ROI of the mandible region for each input data. This region of interest is defined by two corners of the mentioned cube. We use regression to reach the two relative displacement vectors between a reference voxel and the two corners. On the other hand, we choose reference voxels by using a canny algorithm to find those, which have high edge responses in training and testing steps [11]. To have the two displacement vectors from the specified 3D section automatically, we define a localization net, which is a 3D regression FCN shown in Fig. 3.

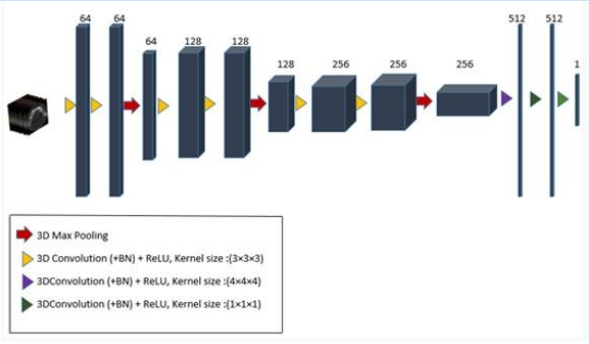

Fig. **3** 3D regression FCN

It is worth mentioning that a deep FCN can learn properties to do previous manual works in an automatic form. It includes two 3D convolutional layers and a pooling layer, which will be repeated for 4 times. The kernel size of convolutional layers is 3×3×3 and the padding process of these layers is similar to each other to prevent having different output sizes in comparison with input size. On the other hand, the function of the pooling layer is halving spatial dimensionality. The input for the localization net is a 3D section in size 64×64 ×64. During the function of layers and repetitions, the final convolutional layer will be converted to a layer with a kernel size of 1×1×1 with 512 features. After this part, we have two convolutions in size 1×1×1, which the last one causes a reduction in the number of output channels to six, and the two mentioned displacement vectors become visible [12].

For training the localization net, we try to optimize the mean squared error loss via Adam solver, and next, we use the intersection of Union loss to train the previous network [13]. Actually, we use IOU loss to have more precise training but we can't use it singly at first and have to follow the mentioned process, because IOU loss needs a basic estimation of corners to make the intersection between the estimated ROI and the real one. It is worth mentioning that during the testing step, we used the kernel density estimation method to have a density function for all the voxels of ROI corners. The maximum value of this function, which is the universal value, will be the predicted location of the mentioned corner.

C. *Segmentation Net*

The goal of this step is the segmentation of the Alveolar canal from the mandible bone. Thus, we do segmentation for the estimated ROI of the mandible from the previous step via 3D U-net (Fig. 4). This neural network, which is like FCN, includes two steps: the encoder and the decoder. The task of the encoder phase is analyzing and learning features of input data and the task of the decoder phase is a segmentation of input data by using information that is accessible from the previous phase. In this network, we have shortcut connections between the encoder and decoder phase in layers that have the same resolution. The kernel size of convolutional layers is 3×3×3 and the kernel size of pooling layers is 2×2×2.

The training process of our U-net [5], which is based on grayscale value, includes two steps. As the first, the U-net is trained for binary segmentation of the mandible and Alveolar canal. To describe precisely, we have differences between pixels of input data, according to the goal region and background, based on their colors. On the other hand, we used the HU value for training too, which is a specific parameter for CBCT images and is similar to the grayscale value with slight differences. Despite the grayscale value, the HU value is absolute so we can interpret grayscale as the HU scale by using some techniques [7]. As the next step, we train U-net for multiclass segmentation to assign classes for each trained weight. It is worth mentioning that we used Adam solver to optimize the weighted cross-entropy loss function. Since the number of background class voxels is more than goal classes, we increase the weights of goal voxels and decrease the backgrounds to make a balance and have better results [14].

For testing this defined net, we give a volumetric image to a trained network and as the next level, we feed overlapped sub-volume patches to the network to have a better viewpoint for the next probable inputs.

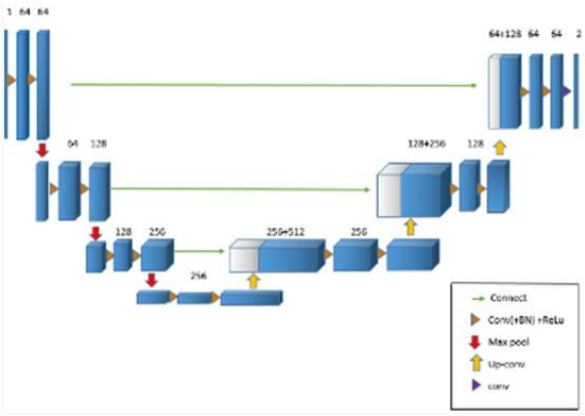

Fig. **4** The architecture of the U-net like Segmentation Net.

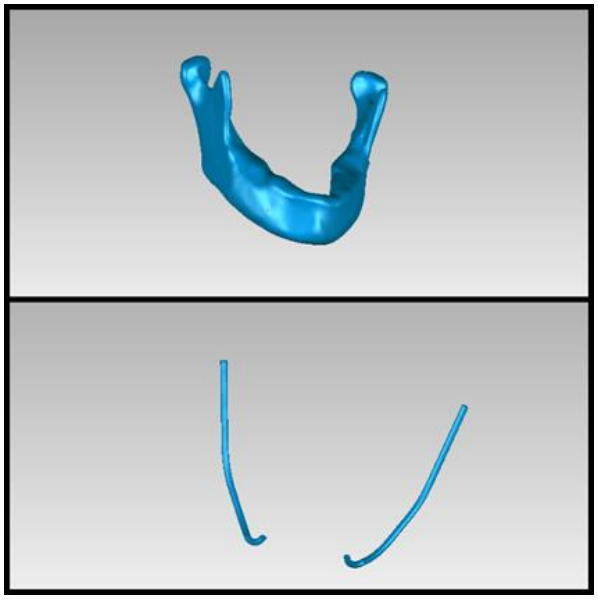

Fig. **5** Segmented Mandible and IAN canal.

D. *GUI*

The goal of this step is to create a program to have the mentioned process in an automatic and efficient mode. So, we represent an exclusive GUI with various options to achieve the best and also quickest performance of previous segmentation steps. On the other hand, we consider the STL format for program output to provide the possibility of having segmented parts in 3D models using 3D bioprinters. To convert the output of our U-Net model into an STL model, we convert the predicted segmentation map from the U-Net model into a binary mask. This process is done by applying a threshold to the segmentation map, setting any pixel above the threshold to 1 (representing the mandible and alveolar canal), and setting any pixel below the threshold to 0 (representing the background). Then we use the binary mask to extract the surface geometry of the mandible and alveolar canal. This is done using various image processing techniques, such as contour detection or morphological operations. The goal is to obtain the outline or contour of the mandible and alveolar canal in the binary mask. Once we have the contour or outline, use a library like numpy-STL to convert the contour into a 3D mesh representation. This library provides functions to create a 3D mesh from a set of vertices and faces. Finally, we export the generated 3D mesh to an STL file using the relevant functions provided by the chosen library. It should be noted that we also used a 3D Mocbioprinter[1] to test the accuracy of GUI outputs as a sample shown in Fig. 6.

Fig. **6** The 3D printed parts of GUI outputs based on defined segmentation net.

III. RESULT AND DISCUSSION

The proposed networks were implemented using Python and experiments were performed on a computer with a single GPU (i.e., NVIDIA GTX 1080 Ti) and Linux Ubuntu 14.04 LTS 64-bit operating system.

[1] https://www.mocstartup.com/

Our Segmentation Net performs well using a defined localization net and we could reach both parts of the mandible bone (main bone and inferior alveolar canal) as shown in Fig. 5. Our approach achieves a mean DC of 86.61% by training 1000 CBCT data and testing 100 as shown in Table 1. For each data, it took about 14 hours to train the localization net, and 24 hours to train the segmentation net. After training, it took on average about 50 seconds to finish the segmentation of one test CBCT data.

TABLE **1**. SEGMENTATION RESULTS

	JC (%)	DC (%)
Inferior alveolar canal	79.35	83.58
Mandible bone	87.89	89.64

IV. CONCLUSION

In this article, we proposed a method based on FCN for a specific two-step net including localization and segmentation to have automatic segmentation of mandible bone. The first mentioned net, which is called the localization net, causes to reach the precise location of the mandible automatically. Since these nets are based on deep learning methods, we compared our defined net with previous works [15], which were somewhat similar to our research, and therefore, we found out that our work has more efficiency with an average DC of 86.61%. In conclusion, we presented a new U-net-based approach as an exclusive program to have automatic segmentation of the inferior alveolar canal from the mandible in a 3D format using CBCT images and also, tested it by 3D printing of GUI outputs. This program can be practical for dentists to reach the exact desired results in less time. It is worth noting that, one area of future work will be finding out the ability of this defined net to recognize different mandible disorders and diseases; for example, different cysts or cancerous masses.

REFERENCES

[1] K. Madan, S. Baliga, N. Thosar, and N. J. J. o. M. Rathi, "Recent advances in dental radiography for pediatric patients: A review," Medicine, Radiology, Pathology & Surgery, vol. 1, pp. 21-25, 2015.

[2] R. Lloréns, V. Naranjo, M. Clemente, M. A. Raya, and S. Albalat, "FC-based Segmentation of Jaw Tissues," in BIOSIGNALS, pp. 409-414, 2010.

[3] D.-J. Kroon, Segmentation of the mandibular canal in cone-beam CT data. Citeseer, 2011.

[4] C. Keatmanee, S. S. Makhanov, K. Kotani, T. Kondo, and S. S. Thongvigitmanee, "Inferior alveolar canal segmentation in cone beam computed tomography images using an adaptive diffusion flow active contour model," 14th IAPR International Conference on Machine Vision Applications (MVA), pp. 57-60, 2015.

[5] O. Ronneberger, P. Fischer, and T. Brox, "U-net: Convolutional networks for biomedical image segmentation," MICCAI, vol. 9351, pp. 234-241, 2015.

[6] M. Wang, J. He, Y. Liu, M. Li, D. Li, and Z. J. I. J. o. B. Jin, "The trend towards in vivo bioprinting," International Journal of Bioprinting, vol. 1, no. 1, 2015.

[7] S. Lee, S. Woo, J. Yu, J. Seo, J. Lee, and C. J. I. A. Lee, "Automated CNN-Based tooth segmentation in cone-beam CT for dental implant planning," IEEE Access, vol. 8, pp. 50507-50518, 2020.

[8] H. Kaur and J. Rani, "MRI brain image enhancement using Histogram equalization Techniques," International Conference on Wireless Communications, Signal Processing and Networking (WiSPNET), vol. 11, pp. 770-773, 2016.

[9] Emer J. Hughes, Tobias Winchman, Francesco Padormo,1 Rui Teixeira,1 Julia Wurie, Maryanne Sharma,1 Matthew Fox,1 Jana Hutter, Lucilio Cordero-Grande,1 Anthony N. Price, Joanna Allsop, Jose Bueno-Conde,1 Nora Tusor,1 Tomoki Arichi,1 A. D. Edwards,1 Mary A. Rutherford, Serena J. Counsell, and Joseph V. Hajnal “A Dedicated Neonatal Brain Imaging System,” Magnetic Resonance in Medicine, vol. 78, pp. 794–804, 2017.

[10] D. Štern, T. Ebner, and M. Urschler, "From local to global random regression forests: Exploring anatomical landmark localization," International Conference on Medical Image Computing and Computer-Assisted

Intervention, Springer. vol. 8674, pp. 221-229, , 2016.

[11] A. Suzani, A. Seitel, Y. Liu, S. Fels, R. N. Rohling, and P. Abolmaesumi, "Fast automatic vertebrae detection and localization in pathological CT scans-a deep learning approach," MICCAI, Springer. vol. 9351, pp. 678-686, , 2015.

[12] K. Simonyan and A. J. a. p. a. Zisserman, "Very deep convolutional networks for large-scale image recognition," arXiv preprint arXiv, vol. 6, pp.1-14, 2014.

[13] J. Yu, Y. Jiang, Z. Wang, Z. Cao, and T. Huang, "Unitbox: An advanced object detection network," Proceedings of the 24th ACM international conference on Multimedia, vol. 127, pp. 516-520, 2016.

[14] Ö. Çiçek, A. Abdulkadir, S. S. Lienkamp, T. Brox, and O. Ronneberger, "3D U-Net: learning dense volumetric segmentation from sparse annotation," MICCAI, vol. 9901, pp. 424-432, 2016.

[15] B. Qiu, J. Guo, J. Kraeima, H.H. Glas, R.J.H. Borra, M.J.H. Witjes, and P.M.A. van Ooijen"Automatic segmentation of the mandible from computed tomography scans for 3D virtual surgical planning using the convolutional neural network," Physics in Medicine & Biology, vol. 64, pp. 175020 (1-13), 2019.

THIS PAGE IS INTENTIONALLY LEFT BLANK.